Correlation Analysis of High-speed Railway Channel Parameters Based on Channel Measurement

YunLing Guo∗, Jianhua Zhang∗, Chi Zhang∗, Lei Tian∗
∗ Key Laboratory of Universal Wireless Communications, Ministry of Education, China
Wireless Technology Innovation Institute, Beijing Univ. of Posts and Telecom., China, 100876
Email: guoyl@bupt.edu.cn

***Abstract*—In this paper, Empirical results characterizing the joint statistical properties of the shadow fading (SF), the root-mean-square (rms) delay spread (DS), and the Ricean K-factor are presented. Measurement data from high-speed railway in viaduct scenario have been analyzed. It is found that a log-normal distribution accurately fits the distribution function of all the investigated parameters. The spatial autocorrelation function of SF, rms DS, and Ricean K-factor can be modeled with an exponential decay function. However, The spatial autocorrelation functions of all three variables are better characterized by a composite of double exponential decaying functions. A positive cross correlation is found between the SF and the Ricean K-factor, while both parameters are negatively correlated with rms DS. All essential parameters required for the implementation of a simulation model considering the joint statistical properties of SF, rms DS, and the Ricean K-factor are provided.**

I. Introduction

As the rapid development of the High-speed Railway, more demands are put forward to the High-speed Railway Wireless Communication System. First of all, channel characteristics of high-speed railway need to be known. And large scale, delay spread (DS), azimuth spread (AS) and doppler effect have been invested in many literatures [1] [2] [3].

However, the correlation properties of shadow fading (SF), Ricean K-factor and the root-mean-square (rms) DS in high-speed railway scenario still remain to be characterized. This includes how the SF, Ricean K-factor and DS vary as the mobile station (MS) moves along a certain route (i.e., autocorrelation properties), mutual dependency between the SF, Ricean K-factor and DS (i.e., cross-correlation properties), etc. Such a description is important for the implementation of realistic network level simulators of modern wideband mobile communication systems in high-speed railway scenarios. Functions that characterize the joint random behavior of SF, Ricean K-factor, and DS are, therefore, extracted from experimental data collected during extensive measurement campaigns. In order to be able to jointly simulate the random behavior of the SF, DS, and Ricean K-factor, it is not sufficient to have knowledge of the distributions and the spatial autocorrelation functions of the three variables. Information on the cross correlation between the variables is also needed. The most convenient method for simulating them on a computer would probably be to generate three random variables. However, this method would result in random variables with zero-cross correlation. To generate correlated variables, we could perform a linear transformation, to obtain a new set of correlated processes.

According to authors, there is only one paper which focuss on the spatial autocorrelation function of SF in high-speed railway scenario for now [4]. In this paper, the dedicated field channel measurement was conducted to investigate the propagation characteristics of high-speed railway. The main contribution of our work is summarized as follows:

(1) Cumulative distribution functions (cdf) of SF, DS and Ricean K-factor are given.

(2) Spatial autocorrelation function of SF, DS and Ricean K-factor and their models are presented.

(3) Cross-correlation coefficients between SF, DS and Ricean K-factor are obtained.

The rest of this paper is organized as follows. Section II describes the measurement system and scenario. In Section III, the procedure of measured data are presented. Section IV presents the results from a high-speed railway viaduct analysis of the measurements, including simple models of the cdf of the parameters under study, the spatial autocorrelation function, and cross-correlation properties. The paper is concluded in Section V.

II. MEASUREMENT CAMPAIGN

The measurement utilized the Elektrobit PropSound Channel Sounder which is described in more details in [1] with a setup of a transmitting antenna and a receiving antenna. A vertical-polarized dipole excites the channel at the transmitter (TX) side, which is on the top of an 8 meters high building. The TX antenna whose location was recorded by Global Positioning System (GPS) device was about 12.8 meters from ground surface. Existing vertical-polarized wideband antenna mounted at rooftop of carriage was used as the receiver (RX) which was about 9 meters high from ground surface. The location of RX was recorded by GPS antenna and saved in the PropSound. The configuration of measurement system parameters are listed in Table. I. The filed channel measurement campaign is performed in ZhengXi high-speed railway with speed of 190-196 Km/h of rural area in the viaduct scenario, which is built highly above the ground and occupies more than fifty percent of all the scenarios in the ZhengXi railway

TABLE I
PARAMETERS OF MEASUREMENT SYSTEM CONFIGURATION

Items	Settings
Transmitting power (dBm)	30.8
Center frequency (GHz)	2.35
Bandwidth (MHz)	50
Code length	127
Antenna type of TX	Dipole
The height of TX (m)	12.8
Height of RX (m)	9
Sample rate (Samples/s)	1968.5

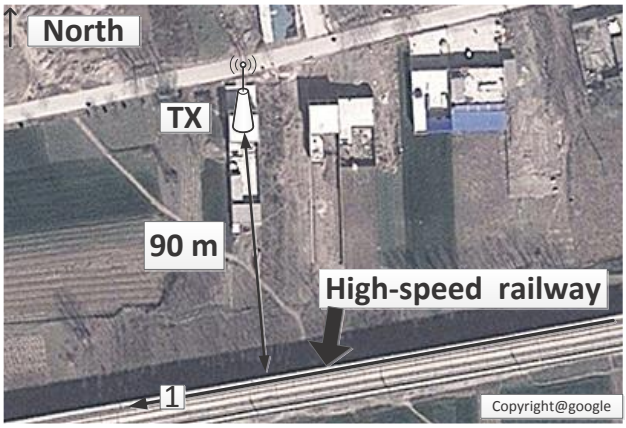

Fig. 1. A bird-eye view of the measurement environment

line. Fig. 1 gives a bird-eye view of the field measurement scenario. The number 1 line with an arrow in Fig. 1 is the route that train traveled. And the distance between the high-speed railway and TX in the horizontal direction is about 90 m. There are a lot of trees between TX and the railway. The heights of trees are 3-7 m. Sample rate of channel was 1968.5 Samples/s which is big enough to get numerous data. What's more, measured route was line-of-sight (LOS) between TX and RX on the whole.

III. DATA PROCESSING

Firstly, we denote the transmitting power and the average receiving power as P_{t} and P_{r}, respectively. And the receiving power can be expressed as

$$P_{\mathrm{r}} = P_{\mathrm{t}} \cdot \overline{\sum_{\tau} \|h(\tau)\|^2}, \tag{1}$$

where $h(\tau)$ is the channel impulse response which can be obtained from measured data and the over bar means the average of the channel samples in a local area [5]. In our data processing, the radius of the circle is chosen to be 10 λ, which is about 1.28 m at 2.35 GHz. λ is the wavelength. P_{r} can also be calculated by the following expression

$$P_r|_{dB} = G - PL - S, \tag{2}$$

where G, PL and S are antenna gain, PL and SF, respectively, all in decibels, $P_r|_{dB}$ is P_{r} in decibels.

The single-slope log-distance model is adopted to estimate the distance dependent path loss, which is of the form

$$PL = A + 10n \log 10(d), \tag{3}$$

where d is the distance between TX and RX in meters, and A is the interception in decibel. Linear regression using a minimum mean square error (MMSE) criterion was utilized to estimate the parameter n and A. The shadowing component in decibel is given by

$$S = G - A - 10n \log 10(d) - P_r|_{dB}. \tag{4}$$

The rms excess DS τ_{rms} is defined as the root mean square of the second central moment of the power delay profile, which can be obtained by

$$\tau_{\mathrm{rms}} = \sqrt{\frac{\sum\limits_{\tau} \tau^2 \cdot P(\tau)}{\sum\limits_{\tau} P(\tau)} - \left(\frac{\sum\limits_{\tau} \tau \cdot P(\tau)}{\sum\limits_{\tau} P(\tau)} \right)^2}, \tag{5}$$

where $P(\tau) = \|h(\tau)\|^2$.

The Ricean K-factor which is defined as the ratio of power of the direct line-of-sight component to the total power of the diffused non-line-of-sight components is estimated by the method of the moment proposed in [6]. Ricean K-factor is obtained as

$$K = \frac{\|V\|^2}{\sigma^2}, \tag{6}$$

where

$$\|V\|^2 = \sqrt{{G_m}^2 - {G_v}^2} \tag{7}$$

and

$$\sigma^2 = G_m - \sqrt{{G_m}^2 - {G_v}^2}. \tag{8}$$

The first moment G_m is the average power gain and the second moment G_v is the RMS fluctuation of power gain.

IV. CORRELATION OF SF, RICEAN K-FACTOR AND DS

A. Spatial Autocorrelation Function of SF, Ricean K-factor and DS

The SF at different distance is extracted as it is introduced above. Fig. 2 is the distribution of SF and the normal distribution fits the samples well. The standard deviation of the normal distribution whose mean is zero is 4.8 dB.

The autocorrelation of SF describe the similarity of SF separated by certain distance. And the SF of two points within the decorrelate distance exits strong correlation. Actually, the autocorrelation of the shadow fading suggests the similarly of the propagation scenario to a certain extent. We use the method in [7] to calculate the autocorrelation of SF. We choose the distance resolution to be about 2.2 m in this paper. The autocorrelation of SF is shown in Fig. 3. The figure shows that the autocorrelation becomes smaller when the separation distance is larger. And the autocorrelation fluctuates around zero value when the separation distance is large enough. We choose the autocorrelation that is never smaller than zero from

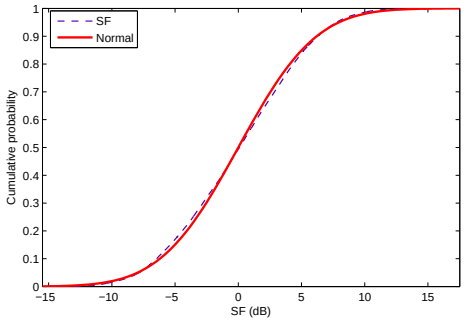

Fig. 2. Cdf of SF in a viaduct

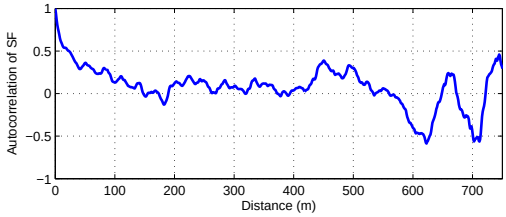

Fig. 3. SF autocorrelation in a viaduct scenario

TABLE II
PARAMETERS OF DISTRIBUTION

Items	SF (dB)	Rms DS ($\log 10(s)$)	Ricean K-factor (dB)
μ	0	-7.04	8.78
σ	4.8	0.54	6.08

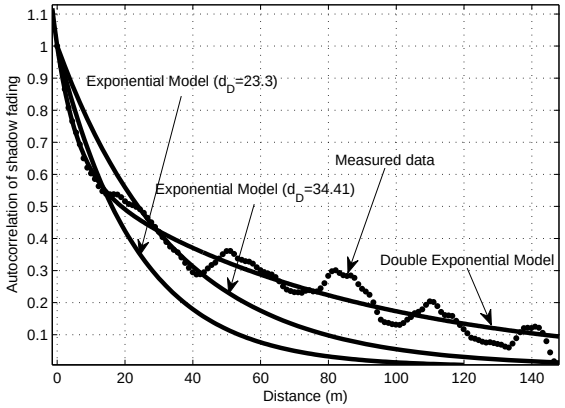

Fig. 4. Comparison of the exponential model and the double exponential model with the measurement correlation of SF

the beginning to analyze the autocorrelation more preciously. Thus the separation distances only within about 147 m are considered in the following proceedings. When analyzing DS and Ricean K-factor, similar method is used.

The decorrelation distance is 34.41 m when the correlation declared to e^{-1} [8] and the value is 23.3 m when the correlation declared to 0.5 in our measurement. The two distances are quite different with the values in [4]. There are two models to model the autocorrelation of SF and their expressions can be written

$$\rho_1(d) = \exp\left(-\frac{d}{d_D}\right), \tag{9}$$

$$\rho_2(d) = \alpha \exp\left(-\frac{d}{d_{D1}}\right) + (1-\alpha)\exp\left(-\frac{d}{d_{D2}}\right), \tag{10}$$

where d_D is the decorrelation distance of the SF, a short decorrelation distance indicates that the SF changes quickly as the RX moves; d is the separation distance; d_{D1} and d_{D2} are the short and long decorrelation distance of the two components, while $\alpha \in [0,1]$ expresses the weighting between the two components. Fig. 4 presents the measured autocorrelation of SF, the exponential model and the double exponential model. The double exponential model compared with the exponential model fits the measured SF autocorrelation better. The long decorrelation distance is 78.9 m and smaller than that in [4]. The short decorrelation distance is 6 m and similar to the value in [4].

Fig. 5(a) shows the empirical cdf of the rms DS in the high-speed railway viaduct scenario. The mean of the calculated RMS DS is 192 ns and greater than that in WINNER II which was calculated by the measurement in rural macrocell scenario at 5.25 GHz [1]. It is found that a normal distribution function provides a good match to the empirical cdf of the rms DS ($\log 10(s)$). The parameters of the distribution are given in Table. II. The spatial autocorrelation function of the rms DS obtained from the high-speed railway in the viaduct scenario is presented in Fig. 6. An exponential decaying function and a double exponential decaying function are plotted for comparison, which accurately match the empirical results. Hence, the autocorrelation function of the DS in high-speed railway viaduct scenario can be modeled according to (9) and (10). d_D is the decorrelation distance of the rms DS. A short decorrelation distance indicates that the DS changes quickly as the MS moves. Thus, and the MS speed give an idea of how fast the radio channels coherence bandwidth changes [9] and, therefore, e.g., also how often RAKE finger allocation and a search should be conducted [10], etc.

In order to get more accurate fast variation of the Ricean K-factor, the estimation interval is set to around 2.5 m which means 100 channnel samples can be obtained one value of Ricean K-factor. Fig. 5(b) shows the empirical cdf of the Ricean K-factor in the high-speed railway viaduct scenario.

TABLE III
SPATIAL DECORRELATION DISTANCE FOR SF, DS, AND RICEAN K-FACTOR IN A VIADUCT SCENARIO

Items	SF	DS	Ricean K-factor
$d_D(0.5)$ (m)	23.3	7	27.7
$d_D\left(e^{-1}\right)$ (m)	34.41	32.7	64.5
d_{D1} (m)	6	0.33	2.8
d_{D2} (m)	78.9	56.3	56.7
α	0.39	0.38	0.15
ITU-R M.2135 (m)	37	50	40

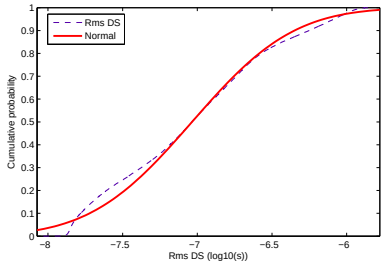

(a)

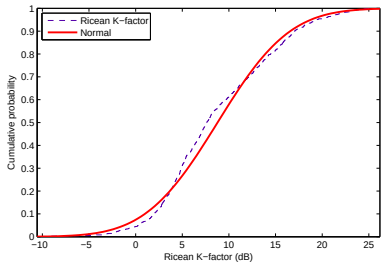

(b)

Fig. 5. (a) Cdf of rms DS (b) Cdf of Ricean K-factor

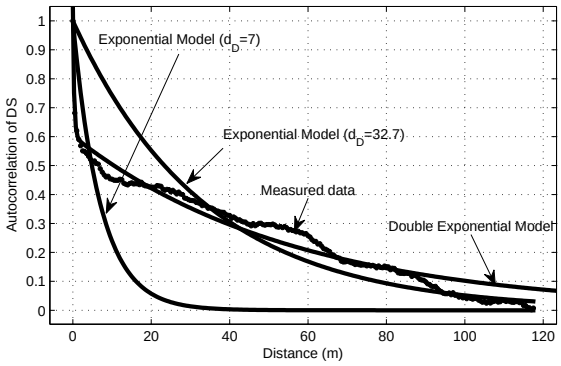

Fig. 6. Comparison of the exponential model and the double exponential model with the measurement correlation of DS

It is found that a normal distribution function provides a good match to the empirical cdf of the Ricean K-factor. The parameters of the distributions are given in Table. II. The spatial autocorrelation function of the rms DS and Ricean K-factor obtained from the high-speed railway in the viaduct scenario are presented in Fig. 6 and Fig. 7, respectively. The double exponential model compared with the exponential model shows better performance to model the autocorrelation of DS and Ricean K-factor.

Their parameters about correlation distance are listed in Table. III. Correlation distance from rural area in LOS case of ITU-R M.2135 (ITU-R M.2135) [11] are also shown in Table. III for comparison. From the table, it can be found that decorrelation distance of SF is similar to that in ITU-R M.2135 and the other two are different from that given in ITU-R M.2135. So it is necessary to have decorrelation distance for high-speed railway scenarios.

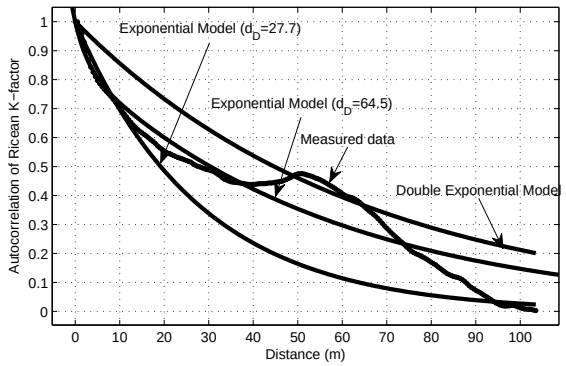

Fig. 7. Comparison of the exponential model and the double exponential model with the measurement correlation of Ricean K-factor

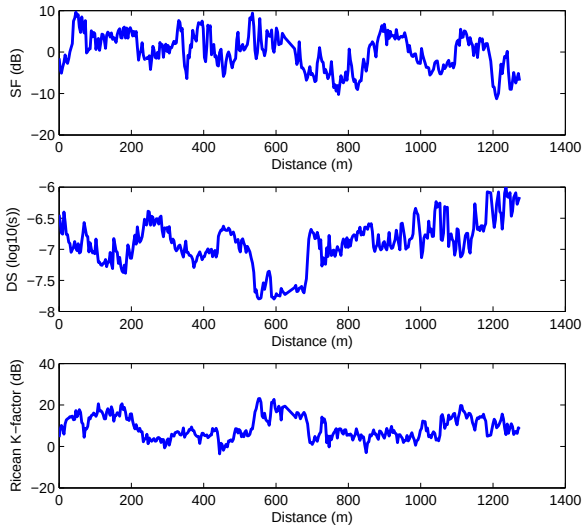

Fig. 8. SF, $\log 10(DS)$ and Ricean K-factor along measured route in high-speed railway viaduct scenario

B. Cross-correlation between SF, Ricean K-factor and DS

The cross-correlation coefficient between a and b is computed according to

$$\rho(a,b) = \frac{\sum_{i=1}^{N} (a(i) - \overline{a})\left(b(i) - \overline{b}\right)}{\sqrt{\sum_{i=1}^{N} (a(i) - \overline{a})^2 \sum_{i'=1}^{N} \left(b(i) - \overline{b}\right)^2}}, \quad (11)$$

where $\overline{a}$ and $\overline{b}$ are the sample means of the sets $\{a(i)\}$ and $\{b(i)\}$ with set size N, respectively.

Fig. 8 pictures the evolution of the logarithmic SF and Ricean K-factor expressed in decibel as well as $\log 10(DS)$ along a measurement route in the high-speed railway viaduct scenario. Based on a visual inspection, there seems to be some correlation between the three variables. A positive cross correlation is observed between SF and the Ricean K-factor as shown in Fig.9 and cross-correlation coefficient is 0.25. It is observed that both SF and Ricean K-factor are negatively

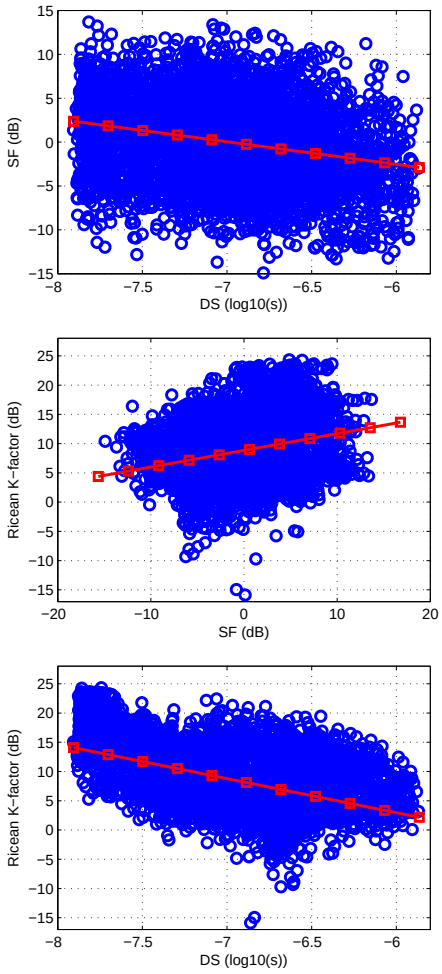

Fig. 9. Scatter plot of SF, $\log 10(DS)$ and Ricean K-factor

correlated with DS as shown in Fig. 9. Their coefficients are -0.26 and -0.51, respectively. The coefficients are quit different from that given in ITU-R M.2135 in LOS case.

V. Conclusion

The joint statistical behavior of the random variables describing SF, the rms DS, and the Ricean K-factor has been characterized based on an analysis of measurement data. These measurement data were collected in high-speed railway viaduct scenario of ZhengXi high-speed railway in China. It is found that a log-normal distribution provides an accurate fit of the empirical cdf of both the SF, the rms DS, and the Ricean K-factor. The spatial autocorrelation function of the three random variables is found to follow an exponential decay. However, the spatial autocorrelation function of all three variables seems to be more accurately modeled with a double exponential decay. The decorrelation distance of SF, DS, and the Ricean K-factor is observed to be identical. The fact that the cdf and the spatial autocorrelation function of the SF, DS, and the Ricean K-factor are identical indicates that the propagation mechanisms leading to these effects are strongly related. A positive cross correlation is found between the SF and the Ricean K-factor, while both parameters are negatively correlated with rms DS. The presented results provide sufficient information to jointly model the random behavior of the SF, the rms DS, and the Ricean K-factor.

Acknowledgment

This research was supported by National Key Technology Research and Development Program of China (2012ZX03001030-004) ,and by Natural Science Foundation of China (61171105, 61032002) ,and by Program for New Century Excellent Talents in University of Ministry of Education of China (NCET-11-0598) ,and by China Mobile Research Institute. The authors would like to thank Weihui Dong from China Mobile Research Institute for his assistance in conducting measurements.

References

[1] *IST-4-027756 WINNER II D1.1.2 v1.2 WINNER II channel models, Feb. 2008. [Online]. Available:http://www.ist-winner.org/WINNER2-Deliverables/D1.1.2.zip*.

[2] L. Liu, C. Tao, J. Qiu, H. Chen, L. Yu, W. Dong, and Y. Yuan, "Position-based modeling for wireless channel on high-speed railway under a viaduct at 2.35 ghz," *IEEE J. Select. Areas Commun.*, vol. 30, no. 4, pp. 834–845, 2012.

[3] R. Parviainen and Pekka, "Results of high speed train channel measurements," European Cooperation in the Field of Scientific and Technical Research, Tech. Rep., 2008.

[4] H. Wei, Z. Zhong, L. Xiong, B. Ai, and R. He, "Study on the shadow fading characteristic in viaduct scenario of the high-speed railway," in *Communications and Networking in China (CHINACOM), 2011 6th International ICST Conference on*, 2011, pp. 1216–1220.

[5] D. Dong, J. Zhang, Y. Zhang, and X. Nie, "Large scale characteristics and capacity evaluation of outdoor relay channels at 2.35 ghz," in *Vehicular Technology Conference Fall (VTC Fall), 2009 IEEE 70th*, sept. 2009, pp. 1 –5.

[6] L. Greenstein, D. Michelson, and V. Erceg, "Moment-method estimation of the ricean k-factor," *Communications Letters, IEEE*, vol. 3, no. 6, pp. 175 –176, june 1999.

[7] Y. Zhang, J. Zhang, D. Dong, X. Nie, G. Liu, and P. Zhang, "A novel spatial autocorrelation model of shadow fading in urban macro environments," in *Proc. IEEE Global Telecommunications Conf. IEEE GLOBECOM 2008*, 2008, pp. 1–5.

[8] A. Algans, K. Pedersen, and P. Mogensen, "Experimental analysis of the joint statistical properties of azimuth spread, delay spread, and shadow fading," *IEEE J. Select. Areas Commun.*, vol. 20, no. 3, pp. 523 –531, April 2002.

[9] B. Sklar, "Rayleigh fading channels in mobile digital communication systems .i. characterization," *Communications Magazine, IEEE*, vol. 35, no. 7, pp. 90–100, 1997.

[10] K. Pedersen and P. Mogensen, "Performance comparison of vector-rake receivers using different combining schemes and antenna array topologies," in *Vehicular Technology Conference, 1999 IEEE 49th*, vol. 1, 1999, pp. 233–237 vol.1.

[11] *Guidelines for Evaluation of Radio Interface Technologies for IMT Advanced, ITU-R Report M.2135, Dec. 2009*.